

Journal of Materials Chemistry C

Accepted Manuscript



This is an *Accepted Manuscript*, which has been through the Royal Society of Chemistry peer review process and has been accepted for publication.

Accepted Manuscripts are published online shortly after acceptance, before technical editing, formatting and proof reading. Using this free service, authors can make their results available to the community, in citable form, before we publish the edited article. We will replace this *Accepted Manuscript* with the edited and formatted *Advance Article* as soon as it is available.

You can find more information about *Accepted Manuscripts* in the [Information for Authors](#).

Please note that technical editing may introduce minor changes to the text and/or graphics, which may alter content. The journal's standard [Terms & Conditions](#) and the [Ethical guidelines](#) still apply. In no event shall the Royal Society of Chemistry be held responsible for any errors or omissions in this *Accepted Manuscript* or any consequences arising from the use of any information it contains.

Cite this: DOI: 10.1039/c0xx00000x

www.rsc.org/xxxxxx

ARTICLE TYPE

Intermediate-paramagnetic phases with a half and a quarter spin entities in fluorinated biphenyl-3,5-diyl bis(*tert*-butyl nitroxides)†

Takuya Konno,^a Hiroki Kudo^a and Takayuki Ishida^{*,a}

Received (in XXX, XXX) Xth XXXXXXXXX 20XX, Accepted Xth XXXXXXXXX 20XX

DOI: 10.1039/b000000x

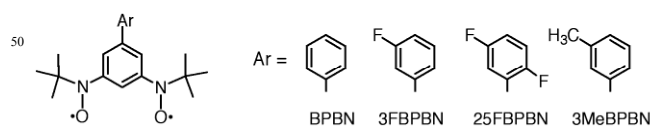
A new ground-triplet biradical, 2',5'-difluorobiphenyl-3,5-diyl bis(*tert*-butyl nitroxide), showed spin-transition-like behaviour at $T_{C\uparrow} = 182$ K and $T_{C\downarrow} = 181$ K. This compound had a quarter of the nominal amount of paramagnetic spins in the low-temperature phase and a half in the high-temperature phase. Another new 3'-monofluoro derivative maintained a half amount of the spins as a single solid phase, which is isomorphous to the high-temperature phase of the difluoro analogue. During the spin transition, a reversible bond formation/cleavage between nitrogen and oxygen atoms takes place at neighbouring nitroxide groups in an intermolecular fashion. These intermediate states emerge during multi-step spin transition from the unsymmetrical biradicals as designed.

Introduction

Various solid-state magnetic switches are of increasing interest for future applications to sensing, memory, display and other devices.¹ Dithiadiazolyls and dithiazolyls attract much attention since they show various spin structures and physical properties in the solid state.² Phenalenyls showing π -dimerization have been studied with respect to transport behaviour and various physical properties.^{3,4} Triphenylimidazolyls also display dramatic photochromism in solution.⁵ Very recently, triazinyls have become a member of organic spin transition materials, and they underwent π -dimerization on cooling.⁶ Such dimerization/degradation solid-state reactions are regulated through the compensation of enthalpic and entropic gains. Namely, dimerized forms are favourable for the enthalpy term while paramagnetic forms for the entropy term. Accordingly, most spin equilibria require minimal atomic dislocation with a small change of enthalpy, leading to spin-transition without any hysteresis.

There have been few known skeletons of organic materials showing facile σ -bond cleavage accompanied by drastic changes of both chromic and magnetic properties. We have reported that the N-O σ -bond forms and cleaves in an intermolecular fashion in the crystals of BPBN derivatives (Scheme 1),^{7,8} where BPBN stands for biphenyl-3,5-diyl bis(*tert*-butyl nitroxide). Another example was found among dialkyl nitroxide family, and 2-azaadamantan-2-oxyl has been reported to show a similar colour and magnetism change.⁹ The BPBN system has an advantage to show an intermediate phase in addition to the usual dia- and paramagnetic regimes.⁸ Furthermore, the bulky *tert*-butyl nitroxide group moves during the transition, which may give a chance to thermal hysteresis. In this report, another intermediate state having a quarter level of paramagnetism will be described for a novel fluorinated BPBN, and this finding can be regarded as a multi-step spin-Peierls-like transition.

Scheme 1. Structural formulas.



Results and discussion

We synthesized two new derivatives, 3'-fluorobiphenyl-3,5-diyl bis(*tert*-butyl nitroxide) (abbreviated as 3FBPBN hereafter) and 2',5'-difluorobiphenyl-3,5-diyl bis(*tert*-butyl nitroxide) (25FBPBN), in which fluorine atoms were introduced at asymmetric positions on the peripheral phenyl ring from our molecular design (Scheme 1). They were prepared in a way different from that of the original BPBN. A key step is the Suzuki cross-coupling reaction¹⁰ of 1-bromo-3,5-bis(*N*-*tert*-butylhydroxylamino)benzene¹¹ with various commercially available aromatic boronic acids. The target biradicals were characterized by means of solution electron paramagnetic resonance (EPR) spectra, which exhibited an unresolved broad line typical of BPBN biradicals.^{7,8}

The magnetic susceptibilities of polycrystalline 3FBPBN and 25FBPBN were measured on a Quantum Design SQUID magnetometer (MPMS-XL7) in a temperature range of 1.8 – 360 K. A half level of paramagnetic spin was observed for 3FBPBN, as indicated by the $\chi_m T$ value (ca. $0.40 \text{ cm}^3 \text{ K mol}^{-1}$) close to the theoretical value of one molar $S = 1/2$ species ($0.38 \text{ cm}^3 \text{ K mol}^{-1}$) (Figure 1). Note that the present BPBN systems can afford room-temperature triplet materials, owing to the intramolecular exchange coupling of the order of $>300 \text{ K}$.^{7,8} The spin-polarization mechanism tells us the ground triplet state in BPBN

compounds, as often verified by *m*-phenylene-bridged biradicals.¹² In the crystal of 3FBPBN, however, an intermediate $S = 1/2$ phase appeared, like 3MeBPBN (3'-methylbiphenyl-3,5-diyl bis(*tert*-butyl nitroxide)).⁸ As the crystallographic analysis of 3FBPBN clarified (see below), just a half of spins is dimerized to form a covalent bond. Consequently, two residual spins appear from every four spins in two molecules. The intermolecular magnetic coupling is much stronger than the intramolecular one. We confirmed that the biradical character was recovered in solution, as indicated by the EPR spectra (Figure S1, Supporting Information). Namely, no 1/1/1 EPR signal typical with a mononitroxide was found, but an unresolved broad line appeared again.

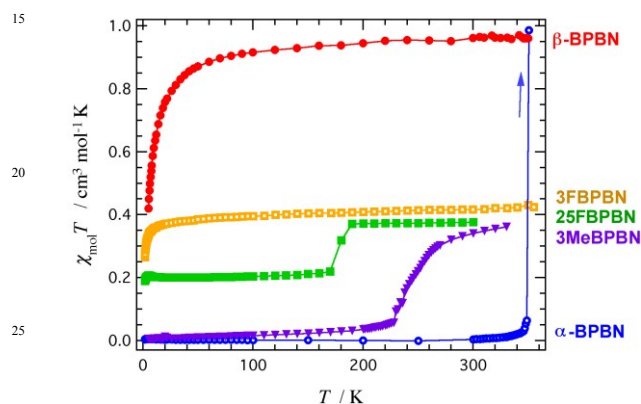


Figure 1. Temperature dependence of $\chi_m T$ for 3FBPBN and 25FBPBN. For comparison, the data of related compounds (BPBN⁷ and 3MeBPBN⁸) are also shown. The solid lines are drawn for a guide to the eye.

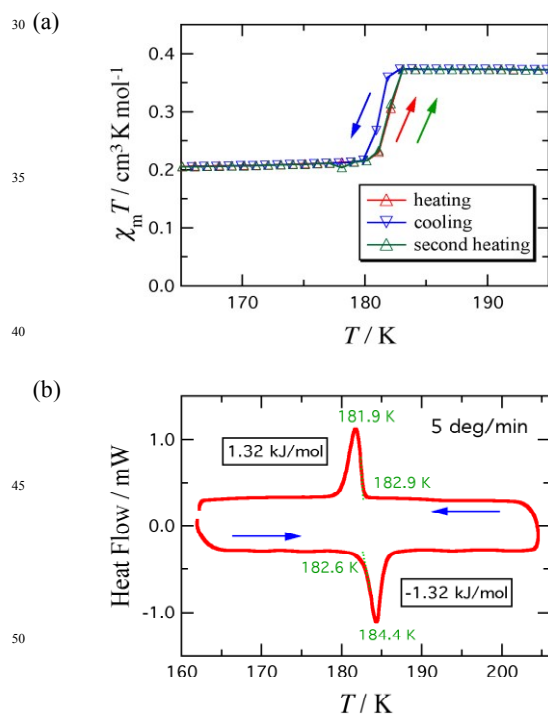


Figure 2. (a) Temperature dependence of $\chi_m T$ for 25FBPBN measured at 5000 Oe. The solid lines are drawn for a guide to the eye. (b) DSC result of 25FBPBN. The peak and onset temperatures are shown. Arrows denote the temperature scan sequences.

An obvious spin-transition-like behaviour was found to occur at $T_{C1} = 182$ K and $T_{C1} = 181$ K for 25FBPBN (Figure 2a as a magnification plot from Figure 1). The transition was completed within a width of 3 K. The interconversion is totally reversible, as observed in repeated experiments. At the high-temperature (HT) phase, the $\chi_m T$ value corresponds to a spin-only value of a doublet species just like 3FBPBN. In the low-temperature (LT) phase below 181 K, a quarter amount of the total spin entity ($\chi_m T = \text{ca. } 0.20 \text{ cm}^3 \text{ K mol}^{-1}$) was recorded, which has never been observed in any BPBN compounds. The onset phase transition temperatures found in the differential scanning calorimetry (DSC) result was consistent with the magnetic results (Figure 2b). The phase transition enthalpy change was determined to be $\Delta_{tr}H = 1.32 \text{ kJ mol}^{-1}$, from which the phase transition entropy change was reduced to $\Delta_{tr}S = 7.3 \text{ J K}^{-1} \text{ mol}^{-1}$. Assuming that two triplet molecules altered to two doublets and one singlet in every four molecules, the spin entropy contribution from the state degeneracy¹³ should be only $(R/2) \ln(3/2) = 1.7 \text{ J K}^{-1} \text{ mol}^{-1}$. Even when a triplet-singlet interconversion is supposed to take place, it would be $(R/4) \ln 3 = 2.3 \text{ J K}^{-1} \text{ mol}^{-1}$. This phase transition accompanies an appreciable latent heat, being responsible for a first-order phase transition of 25FBPBN. Although the thermal hysteresis is substantial in this abrupt transition (Figure 2), the relatively small magnitude of $\Delta_{tr}H$ seems to be related with small displacement of moving atoms in 25FBPBN, in comparison with those of other organic compounds showing polymorph.¹⁴

The crystal structure analysis of 3FBPBN clarified to be isomorphous to the HT phase of 25FBPBN (Table 1). Figure 3a demonstrates the result of 25FBPBN as a representative of this phase (Figure S2, supporting information, shows the X-ray crystal structure of 3FBPBN). The molecules are one-dimensionally arrayed with the nitroxide groups closely interacted. The interatomic distances in 3FBPBN are: 3.7143(13) and 2.3487(19) Å for N1...O1ⁱ and N2...O2ⁱⁱ, respectively, at 163 K, where the symmetry operation codes of *i* and *ii* are $(-x, -y, -z)$ and $(-x, -y+1, -z+1)$, respectively. The latter is 23% shorter than the sum of the van der Waals radii (3.07 Å),¹⁴ whereas the former is apart enough. The corresponding distances in 25FBPBN are as follows: 3.696(4) and 2.429(4) Å for N1...O1ⁱ and N2...O2ⁱⁱ, respectively, at 296 K. Only the latter is short (21% shorter than the sum of the van der Waals radii). The dipolar character indicated by a canonical structure $>N^+-O^-$ is responsible for a head-to-tail dimerization^{9,16} giving a centrosymmetrical (N-O)₂ quadratic motif (Scheme 2). Notable pyramidalization at the N atoms was observed in the dimerized nitroxide sites (Figure 3). Aryl-substituted nitroxides usually possess highly planar nitroxide nitrogen atoms due to π -conjugation.^{11,17} In other words, such pyramidalization is regarded as a fingerprint for dimerized nitroxides. The paramagnetic centre (N1-O1) is best described as a doublet spin because the counterpart (N2-O2) in a molecule practically behaves as being diamagnetic. This scenario will be supported by calculation study (see below).

Scheme 2. Canonical structures after dimerization.

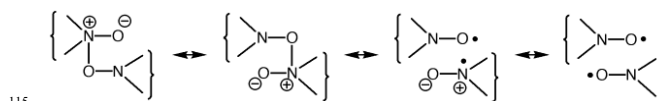
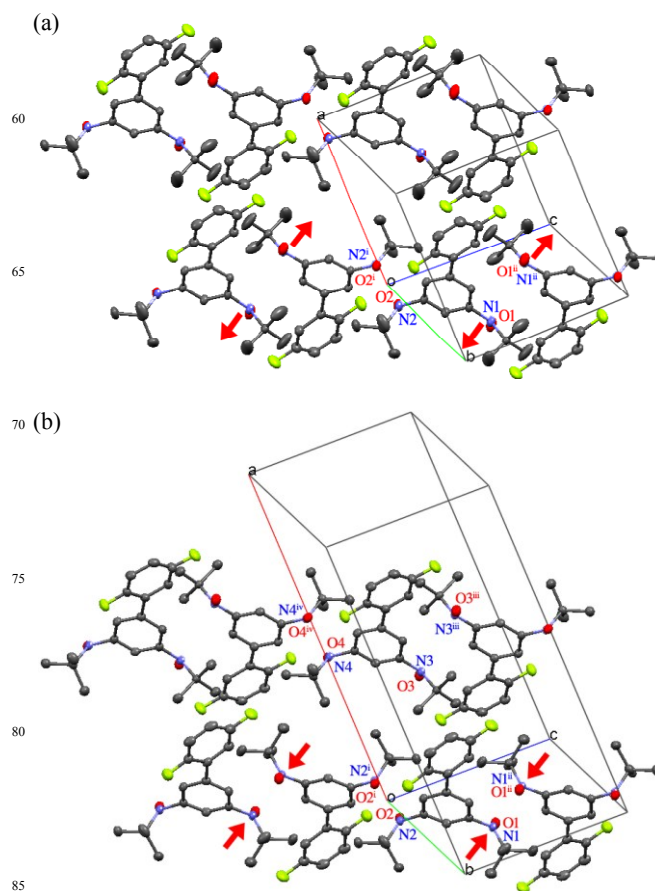
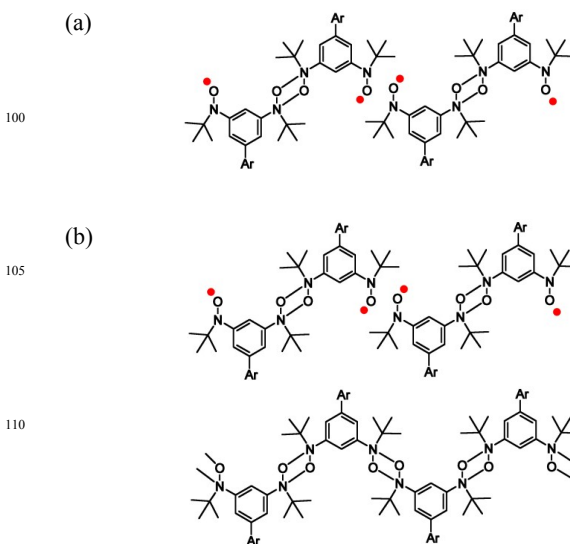


Table 1. Selected crystallographic data for 3FBPBN and the high- and low-temperature phases of 25FBPBN.

Complex	3FBPBN	25FBPBN	
5 Formula	C ₂₀ H ₂₅ FN ₂ O ₂	C ₂₀ H ₂₄ F ₂ N ₂ O ₂	
Formula weight	344.43	362.42	
Crystal Habit	red platelet	red platelet	
Dimension (mm ³)	0.34×0.26×0.10	0.41×0.37×0.12	
Crystal system	triclinic	triclinic	
10 Space group	<i>P</i> -1	<i>P</i> -1	
<i>a</i> (Å)	9.4585(4)	9.549(4)	18.697(10)
<i>b</i> (Å)	10.1452(3)	10.244(5)	10.113(6)
<i>c</i> (Å)	11.4899(5)	12.036(5)	11.965(6)
α (°)	109.5739(13)	111.13(4)	110.81(5)
15 β (°)	95.7112(13)	93.65(3)	95.19(4)
γ (°)	116.1439(9)	116.77(3)	115.19(4)
<i>V</i> (Å ³)	891.86(7)	943.7(8)	1834(2)
<i>Z</i>	2	2	4
<i>D</i> _{calc} (g cm ⁻³)	1.282	1.275	1.312
20 μ (Mo K α) (mm ⁻¹)	0.090	0.096	0.099
unique data	4093	4292	8291
<i>R</i> _{int}	0.0791	0.0507	0.0770
<i>R</i> (<i>F</i>) ^a (<i>I</i> > 2 σ (<i>I</i>))	0.0517	0.0689	0.0596
<i>R</i> _w (<i>F</i> ²) ^b (all data)	0.0515	0.0822	0.0795
25 Goodness-of-fit	1.083	0.997	1.054
<i>T</i> (K)	163	296	100

$$^a R = \sum ||F_o| - |F_c|| / \sum |F_o| \text{ (unit weights)}. \quad ^b R_w = [\sum w(F_o^2 - F_c^2)^2 / \sum w(F_o^2)]^{1/2}.$$

Thanks to the single-crystal-to-single-crystal phase transition, we determined the crystal structures of both phases of 25FBPBN (Figure 3) and furthermore traced them during the transition (Supporting Information, Figures S3 shows the cell parameters as a function of temperature, and Figure S4 demonstrates an animated X-ray crystal structures from 180 to 185 K). The space group *P*-1 was retained in the entire temperature range, but the unit cell was doubled in the *a*-axis direction. From a closer look at the cell lengths, the *a* axis is 1.5% shorter in the LT phase than two times *a* axis in the HT phase. In the HT phase, the unit cell comprises a unique molecule in an asymmetric unit with two independent neighbouring N-O contacts (Figure 3a). On the other hand, there are two crystallographically independent molecules and accordingly four N-O contacts in the LT phase (Figure 3b). The interatomic distances at 100 K are: 2.425(4) Å for N1...O1ⁱⁱ, 2.361(4) Å for N2...O2ⁱ, 3.754(4) Å for N3...O3ⁱⁱⁱ, and 2.329(4) Å for N4...O4^{iv} (the symmetry operation codes of iii and iv are (-*x*+1, -*y*+1, -*z*+1) and (-*x*+1, -*y*, -*z*), respectively). Namely, 3/4 of spins are strongly dimerized. On lowering temperature across *T*_C, one chain became a diamagnetic polymer whilst the other remained a one-dimensional array of paramagnetic dimers. Schematic drawings of the spin-states in the different phases are shown in Scheme 3. There is a half of the nominal spin entity in (a) and a quarter in (b). In any case the residual spin behaves not as a triplet but as two doublet species.

**Figure 3.** X-Ray crystal structures of (a) the high- and (b) low-temperature phases of 25FBPBN. Molecules are one-dimensionally arrayed in a *b*+*c* diagonal direction with relatively short interatomic contacts at the N–O groups. Two “chains” (four molecules each) are shown. Movable N–O groups are marked with arrows. The chains are crystallographically equivalent in (a) while independent in (b).**Scheme 3.** Structural formulas describing the spin-states of (a) 3FBPBN and the high-temperature phase of 25FBPBN and (b) the low-temperature phase of 25FBPBN.

55

115

The density-functional-theory (DFT) molecular orbital (MO) calculation¹⁸ supported that each 25FBPBN molecule potentially possessed the ground triplet state in any phase. The SCF energies of the singlet and triplet states were calculated at the UB3LYP/6-311+G(d,p) level¹⁹ using the molecular geometry at 296 K. We obtained E_{BS} and E_T , where BS stands for the broken symmetry singlet state²⁰ and T for the triplet state. The intramolecular magnetic exchange coupling parameter is defined as $H = -2J_{intra}S_1 \cdot S_2$, and J_{intra} is estimated according to the equation, $J_{intra} = (E_{BS} - E_T) / (\langle S^2 \rangle_T - \langle S^2 \rangle_{BS})$, proposed by Yamaguchi et al.²¹ The ferromagnetic coupling was calculated as $2J_{intra}/k_B = +83.8$ K. The strong intermolecular coupling reduces intramolecular coupling, because on dimerization the N atoms lose the pure $2p_z$ orbital suitable for π -conjugation, as clarified from the crystallographic analysis.

Intermolecular antiferromagnetic coupling was also investigated by supramolecular calculation; two molecules contacted at N1...O1ⁱⁱ were applied to a similar calculation and analysis, after the outer N2-O2 nitroxide radical groups were replaced with hydrogen atoms to reduce calculation cost. Namely, a pair of 2',5'-difluorobiphenyl-3-yl *tert*-butyl nitroxide was subjected to calculation (Figure 4) and the geometry was frozen. From the 296 K structure, the intermolecular parameter J_{inter} was determined to be $2J_{inter}/k_B = -8.6$ K. Very interestingly, the J_{inter} parameter at 100 K was drastically enhanced to as large as $2J_{inter}/k_B = -6.34 \times 10^3$ K, accompanied by the structural change. It is confirmed that the present intermolecular dimer is practically diamagnetic. In short, the calculated intramolecular coupling is stronger in magnitude than the intermolecular one in temperatures higher than the T_C (182 K). In temperatures lower than T_C , the intermolecular coupling becomes dominant.

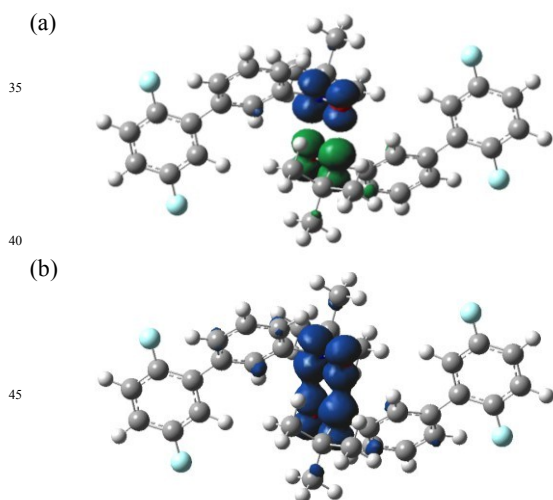


Figure 4. Spin density surfaces of (a) the ground singlet and (b) the excited triplet states of the N1-O1 dimeric model at 100 K. Blue and green surfaces stand for positive and negative spin densities, respectively.

The spin density surfaces are drawn in Figure 4. They approximately display the two singly-occupied MOs. The fluorinated phenyl groups have no appreciable spin density. The meaning of derivatization at the peripheral phenyl ring is to control molecular packing in the crystals.

The present compounds are approximately isomorphous to α -BPBN⁷ and 3MeBPBN.⁸ The substitution at the 2'- and 5'-

positions of the biphenyl skeleton realizes an asymmetric biradical, and there are two independent radical-radical contacts in a unit cell. There seems to be anticooperativity²² along the linear (N-O)₂ array. The notable feature of 25FBPBN is the further differentiation of the chains, giving unequivalent para- and diamagnetic chains. A similar discussion sometimes occurs in multi-step spin-crossover systems,^{1,22} and long-range site orderings showing stripe or other textile-motifs are typical of intermediate spin-transition states.²³ Intermolecular interaction, interchain as well as intrachain, would be required for such a sublattice formation.

An advantage of the use of fluorine atoms may be the ability of hydrogen bonding and dipolar interaction among chains due to the strong electronegativity. Actually, interchain F...H hydrogen bonds were found at F2...C34^v (3.168(4) Å) and F4...C18^{vi} (3.494(5) Å) (the symmetry operation codes for v and vi are (-x+1, -y+2, -z+1) and (x+1, y+1, z+1), respectively). The fluorinated phenyl ring plays a role of an interchain interaction channel. The thermal hysteresis can be thus reasonably comprehended.

Conclusions

Two-step spin-crossover behaviour on iron(II) complexes is well investigated in connection with ternary digit information storage and further applications.¹ Similarly, we have exploited here a series of the BPBN biradical system, and this showed four phases having 0, 1/4, 1/2, and 1 amount of spins in the corresponding phases (Figure 1). Though a 3/4-spin phase is missing so far, quaternary or quinary digit information and computing can be proposed based on the variety of the present phases. These intermediate paramagnetic states emerge during a stepwise spin-Peierls-like transition, and one of the reasons is that the component carries asymmetric radical sites, thanks to a simple molecular design involving asymmetry. The biradicals undergo not only dimerization but also polymerization. Fluorination may afford an attractive intermolecular interaction indispensable for the formation of a sublattice.

Experimental section

Preparation of 3FBPBN. A mixture of 3-fluorophenylboronic acid (0.604 g; 4.3 mmol), 1-bromo-3,5-bis(*N-tert*-butylhydroxylamino)benzene¹¹ (1.43 g; 4.3 mmol), Pd(PPh₃)₄ (0.252; 0.26 mmol), Na₂CO₃ (1.37 g; 13 mmol), dioxane (40 mL), and water (10 mL) was refluxed under nitrogen for 18 h. After usual aqueous work-up using dichloromethane and water, concentration of the organic layer gave faintly yellow powder of the precursory bishydroxylamine of 3FBPBN (0.441 g; 1.3 mmol; yield 30%). The oxidation using a large excess amount of freshly prepared Ag₂O (2 g) was performed in toluene (10 mL) at room temperature for 2 h. After being filtered, recrystallization from dichloromethane-hexane gave needle-like crystals (60%) and prismatic crystals (3%). The latter was found to be a target phase of 3FBPBN. Mp. 82–83°C. The elemental analysis (C, H, N) of the products was carried out on a Perkin Elmer CHNS/O 2400 by a usual combustion method. Anal. Found: C, 69.49; H, 7.47; N, 8.16%. Calcd: C, 69.74; H, 7.32; N, 8.13% for C₂₀H₂₅FN₂O₂. MS(ESI⁺, MeOH) *m/z* 367 (M + Na⁺). IR spectra were recorded

by means of an attenuated total reflection method (ATR) on a Nicolet FT-IR spectrometer. IR (neat, ATR) 2989, 1610, 1212, 896, 791 cm^{-1} . The electron paramagnetic resonance (EPR) was measured on a Bruker X-band ELEXYS spectrometer. EPR (9.4 GHz, toluene, room temp.) $g = 2.0069$, $\Delta B_{\text{p-p}}$ (a peak-to-peak line width) = 2.1 mT.

Preparation of 25FBPBN. According to a similar procedure to that of the 3FBPBN precursor, the coupling of 2,5-difluorophenylboronic acid in place of 3-fluorophenylboronic acid gave the bishydroxylamine of 25FBPBN in 28% yield. The oxidation of the above bishydroxylamine with Ag_2O followed by recrystallization from dichloromethane-hexane afforded 25FBPBN in 40% yield. Mp. 90–92°C. Anal. Found: C, 66.15; H, 6.78; N, 7.64%. Calcd: C, 66.28; H, 6.67; N, 7.73% for $\text{C}_{20}\text{H}_{24}\text{F}_2\text{N}_2\text{O}_2$. MS (ESI^+ , MeOH) m/z 385 ($\text{M} + \text{Na}^+$). IR (neat, ATR) 2989, 1478, 1431, 821, 744 cm^{-1} . EPR (9.4 GHz, toluene, room temperature) $g = 2.0066$, $\Delta B_{\text{p-p}} = 2.2$ mT.

Crystal structure analysis. X-Ray diffraction data of 3FBPBN and 25FBPBN were collected on Rigaku R-axis Rapid and Saturn70 CCD diffractometers with graphite monochromated Mo $\text{K}\alpha$ radiation ($\lambda = 0.71073$ Å). The structures were directly solved by a heavy-atom method and expanded using Fourier techniques in the CRYSTALSTRUCTURE ver 4.0.²⁴ Numerical absorption correction was used. The thermal displacement parameters of non-hydrogen atoms were refined anisotropically and those of hydrogen atoms were treated isotropically. Selected crystallographic data are listed in Table 1. CCDC numbers 1052184-1052186.

Physical property measurements. Magnetic susceptibilities of 3FBPBN and 25FBPBN were measured on a Quantum Design MPMS-XL SQUID magnetometer with a static field of 0.5 T in a temperature range 1.8 - 300 K. The magnetic responses were corrected with diamagnetic blank data of the sample holder measured separately. The diamagnetic contribution of the sample itself was estimated from Pascal's constants. The differential scanning calorimetry (DSC) of 25FBPBN was performed on a Rigaku Thermo Plus DSC 8230.

DFT calculation. Density-functional-theory molecular orbital calculations were performed on the Gaussian03 program.¹⁸ Unrestricted B3LYP methods with the Becke exchange functional and the Lee–Yang–Parr correlation functional were applied.¹⁹ The 6-311+G(d,p) basis set was selected. The convergence criterion was 10^{-7} a.u. The Hartree-Fock energies of the singlet states were obtained according to the broken symmetry method.^{20,21} Single-point energy calculation was performed by use of the geometrical parameters determined by means of the X-ray crystallography.

Notes and references

^a Department of Engineering Science, The University of Electro-Communications, Chofu, Tokyo 182-8585, Japan. Fax: 81 42 443 5501; Tel: 81 42 443 5501; E-mail: ishi@pc.uec.ac.jp

† Electronic Supplementary Information (ESI) available: X-band EPR spectra of 3FBPBN and 25FBPBN measured in toluene solution at room temperature and 145 K, the crystal structure of 3FBPBN, the cell parameters as a function of temperature for 25FBPBN and an animated gif during the phase transition of 25FBPBN. CCDC 1052184-1052186 contain the supplementary crystallographic data for 3FBPBN (163 K) and 25FBPBN (100 and 296 K). These data can be obtained free of charge via <http://www.ccdc.cam.ac.uk/conts/retrieving.html>, or from the Cambridge

Crystallographic Data Centre, 12 Union Road, Cambridge CB2 1EZ, UK; fax: (+44) 1223-336-033; or e-mail: deposit@ccdc.cam.ac.uk. See DOI: 10.1039/b000000x/

- (a) P. Gütlich and H. A. Goodwin Eds. *Spin Crossover in Transition Metal Compounds I, II, and III*; Springer-Verlag: Berlin, 2004; (b) P. Gütlich, A. Hauser and H. Spiering, *Angew. Chem., Int. Ed. Engl.*, 1994, **33**, 2024; (c) M. A. Halcrow, Ed. *Spin-crossover Materials: Properties and Applications*; John Wiley & Sons: Chichester, UK, 2013; (d) M. A. Halcrow, *Polyhedron*, 2007, **26**, 3523.
- (a) W. Fujita, K. Awaga, H. Matsuzaki and H. Okamoto, *Science*, 1999, **286**, 261; (b) W. Fujita, K. Kikuchi and K. Awaga, *Angew. Chem. Int. Ed.*, 2008, **47**, 9480; (c) K. Lakin, S. M. Winter, L. E. Downie, X. Bao, J. S. Tse, S. Desgreniers, R. A. Secco, P. A. Dube and R. T. Oakley, *J. Am. Chem. Soc.*, 2010, **132**, 16212; (d) S. Vela, M. Deumal, M. Shiga, J. J. Novoa and J. Ribas-Arino, *Chem. Sci.*, 2015, doi: 10.1039/C4SC03930K.
- (a) Y. Morita, S. Suzuki, K. Sato and T. Takui, *Nature Chem.*, **2011**, **3**, 197; (b) S. Suzuki, Y. Morita, K. Fukui, K. Sato, D. Shiomi, T. Takui and K. Nakasuji, *J. Am. Chem. Soc.*, **2006**, **128**, 2530; (c) A. Ueda, H. Wasa, S. Suzuki, K. Okada, K. Sato, T. Takui and Y. Morita, *Angew. Chem. Int. Ed.*, **2012**, **51**, 6691.
- (a) S. K. Pal, P. Bag, A. Sarkar, X. Chi, M. E. Itkis, F. S. Tham, B. Donnadieu and R. C. Haddon, *J. Am. Chem. Soc.*, 2010, **132**, 17258; (b) M. E. Itkis, X. Chi, A. W. Cordes and R. C. Haddon, *Science*, 2002, **296**, 1443; (c) Z. Mou, K. Uchida, T. Kubo and M. Kertesz, *J. Am. Chem. Soc.*, 2014, **136**, 18009.
- (a) Y. Kishimoto and J. Abe, *J. Am. Chem. Soc.*, **2009**, **131**, 4227; (b) S. Hatano, T. Horino, A. Tokita, T. Oshima and J. Abe, *J. Am. Chem. Soc.*, **2013**, **135**, 3164; (c) K. Mutoh, M. Sliwa and J. Abe, *J. Phys. Chem. C*, **2013**, **117**, 4808.
- C. P. Constantinides, A. A. Berezin, G. A. Zissimou, M. Manoli, G. M. Leitus, M. Bendikov, M. R. Probert, J. M. Rawson and P. A. Koutentis, *J. Am. Chem. Soc.*, 2014, **136**, 11906.
- (a) G. Kurokawa, T. Ishida and T. Nogami, *Chem. Phys. Lett.*, 2004, **392**, 74; (b) H. Nishimaki, S. Mashiyama, M. Yasui, T. Nogami and T. Ishida, *Chem. Mater.*, 2006, **18**, 3602.
- H. Nishimaki and T. Ishida, *J. Am. Chem. Soc.*, 2010, **132**, 9598.
- S. Matsumoto, T. Higashiyama, H. Akutsu and S. Nakatsuji, *Angew. Chem. Int. Ed.*, 2011, **50**, 10879.
- A. Suzuki, *Angew. Chem. Int. Ed.*, 2011, **50**, 6722.
- F. Kanno, K. Inoue, N. Koga and H. Iwamura, *J. Phys. Chem.*, 1993, **97**, 13267.
- (a) H. Iwamura, *Adv. Phys. Org. Chem.*, 1990, **26**, 179; (b) A. Rajca, *Chem. Rev.*, 1994, **94**, 871; (c) T. Ishida and H. Iwamura, *J. Am. Chem. Soc.*, 1991, **113**, 4238; (d) K. Mukai, H. Nagai and K. Ishizu, *Bull. Chem. Soc. Jpn.*, 1975, **48**, 2381; (e) N. M. Gallagher, A. Olankitwanit and A. Rajca, *J. Org. Chem.*, 2015, **80**, 1291.
- R. Boca, *Theoretical Foundations of Molecular Magnetism Vol. 1 of Current Methods in Inorganic Chemistry*, Elsevier, Amsterdam, 1999.
- (a) N. Sarier and E. Onder, *Thermochim. Acta*, 2012, **540**, 7; (b) V. Stilianovic and B. Kaitner, *Cryst. Growth Des.*, 2013, **13**, 1703.
- A. Bondi, *J. Phys. Chem.*, 1964, **68**, 441.
- (a) Y. Kanzaki, D. Shiomi, K. Sato and T. Takui, *J. Phys. Chem. B*, 2012, **116**, 1053; (b) T. Ishida, M. Ooishi, N. Ishii, H. Mori and T. Nogami, *Polyhedron*, 2007, **26**, 1793; (c) D. Marsh, *J. Mag. Res.*, 2008, **190**, 60.
- A. Okazawa, Y. Nagaichi, T. Nogami and T. Ishida, *Inorg. Chem.*, 2008, **47**, 8859.
- Gaussian 03, Revision C.02*, M. J. Frisch, G. W. Trucks, H. B. Schlegel, G. E. Scuseria, M. A. Robb, J. R. Cheeseman, J. A. Montgomery, Jr., T. Vreven, K. N. Kudin, J. C. Burant, J. M. Millam, S. S. Iyengar, J. Tomasi, V. Barone, B. Mennucci, M. Cossi, G. Scalmani, N. Rega, G. A. Petersson, H. Nakatsuji, M. Hada, M. Ehara, K. Toyota, R. Fukuda, J. Hasegawa, M. Ishida, T. Nakajima, Y. Honda, O. Kitao, H. Nakai, M. Klene, X. Li, J. E. Knox, H. P. Hratchian, J. B. Cross, V. Bakken, C. Adamo, J. Jaramillo, R. Gomperts, R. E. Stratmann, O. Yazyev, A. J. Austin, R. Cammi, C. Pomelli, J. W. Ochterski, P. Y. Ayala, K. Morokuma, G. A. Voth, P. Salvador, J. J. Dannenberg, V. G. Zakrzewski, S. Dapprich, A. D. Daniels, M. C. Strain, O. Farkas, D. K. Malick, A. D. Rabuck, K. Raghavachari, J. B. Foresman, J. V. Ortiz, Q. Cui, A. G. Baboul, S.

- Clifford, J. Cioslowski, B. B. Stefanov, G. Liu, A. Liashenko, P. Piskorz, I. Komaromi, R. L. Martin, D. J. Fox, T. Keith, M. A. Al-Laham, C. Y. Peng, A. Nanayakkara, M. Challacombe, P. M. W. Gill, B. Johnson, W. Chen, M. W. Wong, C. Gonzalez and J. A. Pople, Gaussian, Inc., Wallingford CT, USA, 2004.
- 19 (a) A. D. Becke, *J. Chem. Phys.*, 1993, **98**, 5648; (b) C. Lee, W. Yang and R. G. Parr, *Phys. Rev. B*, 1998, **37**, 785.
- 20 E. Ruiz, J. Cano, S. Alvarez and P. Alemany, *J. Comput. Chem.*, 1999, **20**, 1391.
- 10 21 M. Nishino, S. Yamanaka, Y. Yoshioka and K. Yamaguchi, *J. Phys. Chem. A*, 1997, **101**, 705.
- 22 Y. Garcia, O. Kahn, L. Rabardel, B. Chansou, L. Salmon and J. P. Tuchagues, *Inorg. Chem.*, 1999, **38**, 4663; J. A. Real, A. B. Gaspar, V. Niel, M. C. Munoz, *Coord. Chem. Rev.*, 2003, **236**, 121.
- 15 23 (a) D. Chernyshov, M. Hostettler, K. W. Tornroos and H.-B. Burgi, *Angew. Chem. Int. Ed.*, 2003, **42**, 3825; (b) D. L. Reger, C. A. Little, V. G. Young, Jr. and M. Pink, *Inorg. Chem.*, 2001, **40**, 2870; (c) M. Griffin, S. Shakespeare, H. J. Shepherd, C. J. Harding, J. F. Letard, C. Desplanches, A. E. Goeta, J. A. K. Howard, A. K. Powell, V.
- 20 Mereacre, Y. Garcia, A. D. Naik, H. Muller-Bunz and G. G. Morgan, *Angew. Chem. Int. Ed.*, 2011, **50**, 896; (d) K. D. Murnaghan, C. Carbonera, L. Toupet, M. Griffin, M. M. Dirtu, C. Desplanches, Y. Garcia, E. Collet, J.-F. Letard and G. G. Morgan, *Chem. Eur. J.*, 2014, **20**, 5613.
- 25 24 *CRYSTALSTRUCTURE, version 4.0*, Rigaku/MSC, The Woodlands, TX 77381, USA, 2010.

Intermediate-paramagnetic phases with a half and a quarter spin entities in fluorinated biphenyl-3,5-diyl bis(*tert*-butyl nitroxides)

Takuya Konno, Hiroki Kudo, and Takayuki Ishida*

*Department of Engineering Science, The University of Electro-Communications,
Chofu, Tokyo 182-8585, Japan*

A Table of Contents Entry.

A ground-triplet molecule 25FBPBN showed spin-transition-like behaviour with a small hysteresis, while 3FBPBN maintained a single phase.

